

# Automatic Segmentation of Pulmonary Lobe Using Marker Based Watershed Algorithm

Ulaganathan Gurunathan<sup>#1</sup>, Brindha Manohar<sup>\*2</sup>, Banumathi Arumugam<sup>#3</sup>, Vijayakumari Pushparaj<sup>#4</sup>,  
Balachandar<sup>#5</sup>

<sup>#1</sup>Department of Oral & Maxillofacial surgery, Best Dental Science College, Madurai, India.

<sup>\*2</sup>Department of ECE, Thiagarajar college of Engineering, Madurai, India.

<sup>#3</sup>Department of ECE, Thiagarajar College of Engineering, Madurai, India.

<sup>#4</sup>Department of ECE, Thiagarajar college of Engineering, Madurai, India.

<sup>#5</sup>Department of ECE, Thiagarajar College of Engineering, Madurai, India.

**ABSTRACT**— Segmentation is an important process in the field of medical imaging, as it can provide detailed information of an image. In this work, segmentation of pulmonary lobe is carried out which is useful for the clinical interpretation of CT images, to access the early presence and the characterization of several lung diseases. This segmentation process is challenging for severely diseased lung or lung with incomplete fissures. Existing methods highly rely on the detection of fissures whereas, this technique becomes less reliable in cases of abnormalities. In order to overcome this, automatic segmentation of the lung lobe is performed using marker based watershed algorithm. The proposed algorithm consists of five stages. The first stage is the segmentation of blood vessel using thresholding. The second step involves the segmentation of fissures based on the Eigen values of the Hessian matrix. The third stage is the segmentation of bronchial tree through region growing. Fusing these three results to form the cost image is the fourth step. The final stage is the application of watershed algorithm for the cost image. The run time, mean and accuracy calculation were performed and the results showed that the proposed method possess minimum runtime, mean distance when compared with the existing methodology.

**KEYWORDS**— fissure, lung lobe, cost image, watershed transform, hessian matrix

## I. INTRODUCTION

The human lungs possess five lobes which are separated by visceral pleura termed as pulmonary fissure. The three lobes in the right lung namely, right upper, right middle and right lower are separated by right minor fissure and right major fissure respectively. The two lobes in the left lung namely, left upper and left lower are separated by left major fissure. Fig.1 represents the structure of lung. Lung lobe segmentation is important in clinical applications especially for diagnosis and treatment of lung diseases. The location and distribution of pulmonary diseases are important parameters for the selection of a suitable treatment. Locally distributed emphysema can be treated more effectively by lobar volume resection than homogeneously distributed emphysema. Another application is quantitative monitoring of pulmonary diseases such as emphysema or fibrosis. Progression of the diseases can be determined accurately through the lobe wise analysis.

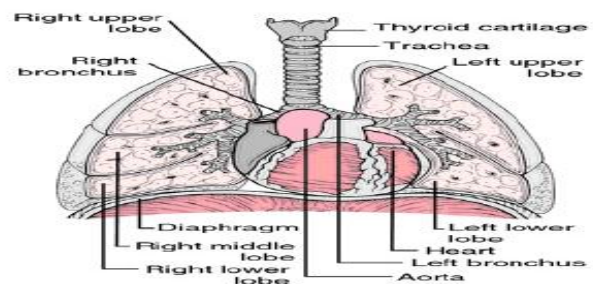


Fig.1 Structure of lung

The visualization of entire lung within few second is possible through Computed Tomography (CT). Manual segmentation is highly time consuming, since 400 slices with sub-millimeter resolution in each direction is taken in typical scans with high anatomical details. Thus there is a great requirement for automatic segmentation of lung lobe. Due to the variations in anatomical structure of the lobes and incomplete fissure, segmentation of lung lobes is difficult. There are two main reasons where the fissure becomes incomplete or unrecognizable, they are: pathologies can deform the lobe and thus the fissure becomes unrecognizable and due to normal lung parenchyma fissures are often not complete. Radiologists, in such cases acquire information from the blood vessel and bronchial tree to infer the lobar boundaries.

The literature shows that, there are number of methods proposed for the lung lobe segmentation. Van Rikxoort et al., presented a method for lobar fissure segmentation [1] in CT data. For patients with complete pulmonary fissures, a segmentation of these fissures is sufficient to obtain lung lobe segmentation. Since in many cases fissures are incomplete, additional processing steps are required to obtain lobe segmentation. Nevertheless, the segmentation of visible fissures offers a good basis for lobe segmentation and can also be used for other purposes with clinical relevance such as quantifying the completeness of the fissures, which is an important feature for treatment planning of patients with emphysema. In [2], pulmonary lobes and segments were found by supervised classification. The fissures were enhanced and segmented by the eigenvalues and eigenvectors of the Hessian matrix. Subsequently, features such as the position relative to the fissures provided a labeling to a pulmonary lobe for every voxel inside the lung. The second lobe segmentation method by van Rikxoort et al., is an automatic multi-atlas approach [3]. First, the lungs, fissures, and bronchi were segmented automatically and combined into one cost image. A fast registration of this result with a set of five atlases with complete fissures gave the best matching atlas that was chosen for a fine registration to get the lobe segmentation result. Atlas-based methods are generally time consuming, segmentation of one case took 2 hours on an average. Another disadvantage of this approach was that scans with lobar shapes not represented in the atlas set were unlikely to be segmented correctly. Ukil and Reinhardt presented pulmonary lobe segmentation [4]. In the first step, the lobes were segmented by a watershed transformation based on a distance map of the vasculature and markers from the labeled bronchi tree. In the second step, 3-D optimal surface detection was performed in a region of interest (ROI) around the initial segmented fissures to refine the lobe boundaries. As a last step, incomplete fissures were extrapolated based on a fast-marching method. Pu.et.al. proposed an automatic lobe segmentation [5] method that started by detecting plane patches in sub volumes in the lungs. From these patches the pulmonary fissures were inter- and extrapolated using implicit radial basis functions. Based on the implicit

functions representing the fissures, the lungs were divided into five lobes. No anatomical information of bronchi or

vessels were taken into account in cases of incomplete fissures. Segmentation took on an average 25 min for one case whose slice thickness is around 0.625–1.25mm.

This work proposes an automatic lung lobe segmentation method that uses information from automatic segmentations of the bronchi, vessels, and visible fissures in a 3-D watershed transformation to be both robust against incomplete fissures and accurate at visible fissures. Although all previously published lobe segmentation methods described above were evaluated, it is not possible to compare the results directly because evaluation was performed on different datasets and with different evaluation measures (volume overlap, distance to the fissures, visual inspection).

## II. METHODOLOGY

A lobe segmentation method is developed which combines anatomical information from the lungs, vessels, airways, and lobar fissures [6] to obtain the lobes using a watershed-based segmentation method. Fig.2 provides an overview of the segmentation process. The method starts by segmenting the lungs, vessels, airways, and fissures, which are later combined into one cost image for the watershed segmentation process.

### A. Preliminary Segmentations

1) *Pulmonary Vessels*: Based on the assumption that there are usually no major vessels at the lobar boundaries, the distance to the pulmonary vasculature is a suitable feature to detect lobar boundaries. To quantify the absence of vessels at the lobar boundaries, a coarse segmentation of the pulmonary vasculature is sufficient. There is high contrast between blood vessels and lung parenchyma that enables a coarse segmentation of the pulmonary blood vessels by thresholding the data inside the lung region. The goal is to include as many vessels as possible but exclude fissures and other dense structures. Before thresholding, a downscaling with clamping is applied to reduce memory requirements. Using (1) the dataset is scaled down to the 8-bit range, where  $L$  is the lung mask  $v$  is the image pixel.

$$V_{ds} = \begin{cases} \max(0, \min(255, (v_{orig} + 1024)/4)), & v \in L \\ 255, & \text{otherwise} \end{cases} \quad (1)$$

The resulting dataset is thresholded to receive the vessel-mask  $V$

$$V = 130 \leq V_{ds} \leq 255 \quad (2)$$

As reported by Bianca lassen, the intensity values of pulmonary vessels lie within 130 to 255, [7]. Thus fixed threshold of 130 was empirically estimated on an independent dataset and proved to be a good trade-off between sensitivity and specificity.

2) *Pulmonary Fissures*: The first step of the fissure segmentation process is an enhancement of the fissures based on the eigenvalues of the Hessian matrix that gives a fissure probability for each voxel [7,8].

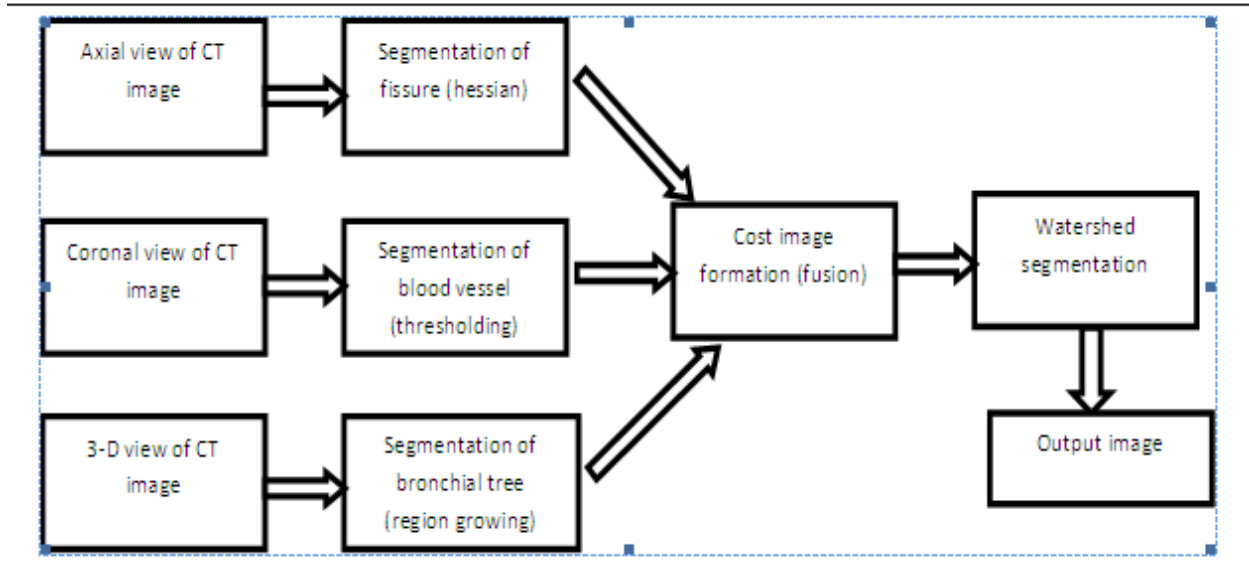


Fig. 2 Pipeline of the proposed method

The relation between the eigenvalues of the Hessian matrix describes the local image structure. The proposed fissure enhancement approach characterizes fissure voxels as:  $0 \ll |\lambda_3| < \delta$  and  $|\lambda_2| \approx 0$ , where  $\delta$  describes the  $|\lambda_3|$  value for vessels.  $\delta$  is introduced to discriminate between fissures and vessels since vessels usually exhibit a larger  $|\lambda_3|$  compared to fissures because of their stronger image contrast. From these characteristics two features are derived using (3) and (4).

$$F_{\text{structure}} = \Theta(-\lambda_3) \exp [-(\lambda_3 - \alpha)^6 / (\beta^6)] \quad (3)$$

$$F_{\text{sheet}} = \exp [-(\lambda_2)^6 / (\beta^6)] \quad (4)$$

$F_{\text{structure}}$  rates the strength of the image structure. Because the intensity of the image structure varies both between patients and also within a single dataset, a wide interval of image intensities for high fissure probability is defined. To estimate suitable values for  $\alpha$  and  $\beta$ ,  $\lambda_3$  values for five other datasets have been analyzed. From this analysis it is revealed that  $\lambda_3$  value lies between 20 and 80. Vessels which are high intensity component possess high  $\lambda_3$ , whereas smaller vessels show  $\lambda_3$  value around 60.  $\Theta(-\lambda_3)$  is the Heaviside function that sets  $F_{\text{structure}}$  value to 0 (i.e., a dark structure on a bright background), when  $\lambda_3 \geq 0$ . Generally in medical application sensitivity is preferred

over specificity, hence  $\alpha = 50$  and  $\beta = 35$  is chosen for the distribution function of  $F_{\text{structure}}$ . Therefore the voxels with  $\lambda_3$  value 30 to 70 is considered to be high fissure probability voxels and voxels having  $\lambda_3$  value greater than 100 are eliminated from segmentation. The  $F_{\text{sheet}}$  differentiates between the sheet structure and other structure like nodules, vessels etc., since the vessels and nodules have larger  $\lambda_2$  values compared with the fissure.

Similar to  $\alpha$  and  $\beta$  values  $\gamma$  is also determined from the five other datasets which is not used for evaluation in this paper. Thus voxels with the  $\lambda_2$  value greater than 30 are assigned a probability 0, and eliminated from the

segmentation. The two features  $F_{\text{sheet}}$  and  $F_{\text{structure}}$  should be in the range [0, 1]. These two features are combined

using (5), to form the similarity measure  $S_{\text{fissure}}$ . The result of fissure enhancement is that each voxel should have a value in the range of [0, 1].

$$S_{\text{fissure}} = F_{\text{structure}} * F_{\text{sheet}} \quad (5)$$

The result of fissure enhancement is used for the segmentation of pulmonary fissure which is used for the watershed lobe segmentation. A mask  $C$ , which describes all the candidate voxels, is formed, such that each voxel satisfies two constraints. One is the minimum fissure similarity and the other demands an intensity value within the specified range.

$$C = [S_{\text{fissure}} > 0.1] \wedge [I_v < (\mu_{\text{vessel}} - 2\sigma_{\text{vessel}})] \quad (6)$$

Where, the  $\mu_{\text{vessel}}$  and  $\sigma_{\text{vessel}}$  are the mean and standard deviation of the vessels, which are determined from the histogram analysis of the segmented vessels.  $I_v$  represents intensity value of each pixel.

3) *Bronchi*: Lobes are separately supplied sub-trees of bronchial tree. Hence distance to the bronchial tree is suitable feature to detect lobar boundaries. In CT images, the airway lumen is dark and separated from the other parenchymal tissue by thin airway a wall structure that is brighter. In CT images, the segmentation of airways is challenging, since the parenchymal fissure often has same Hounsfield Unit values similar to Lumen. Also the Partial Volume Effect and noise obscure the airway walls. Two pre-processing steps are applied to overcome these problems. First one is Gaussian smoothening [9]. This smoothening is applied to the image to reduce the noise, even though this blurring increases the partial volume related problems. The second is the, enhancement of the bronchial tree [10]. The enhancement filtering is applied to the blurred image. Due to partial volume effects and additional Gaussian blurring the lumen of small airways appear brighter than normal air. The importance of bronchi enhancement filtering is to detect the voxels that are surrounded by dense circular structure such as bronchi. Finally to segment the bronchial tree, region growing algorithm [11],[12], is used after applying thresholding to the enhanced image. The region growing is initialized by detecting the trachea pixels as the seed point.

*B. Watershed Lobe Segmentation*

The various anatomical features that are extracted from segmentation of fissures, blood vessel and bronchial tree are combined into cost image [13]. This cost image is formed by multiplicative method. To get good coverage of the lobe area, the markers created should be distributed throughout the lobes. The various sub trees belonging to the various lobes and other lobar segments are estimated to generate markers. For the generation of the markers first a directed graph is generated from the bronchial tree with trachea as the root [14]. The two sub trees with maximum separation are separated into two different branches. Similar to this separation, first the lung is divided into left and right lung[15], and then the sub trees are further divided into various lobes. Thus the labeled airway is used to determine the marker position for the watershed. Next step is to convert the labeled vessels, bronchial tree and fissure as marker for the watershed algorithm [7]. The border between lobes that is obtained as a result of watershed segmentation is not smooth. This is because of the local variations in the cost image. Two majority filters are applied in row wise manner to smooth the resultant segmented image.

III. RESULTS AND DISCUSSION

The algorithm is implemented in MATLAB 2010a on windows 7 environment. And it is tested with dataset containing six images of different views. Fig.3(a), 3(b) shows the images with incomplete fissures. The sample image Fig.3 (a), considered here is of size (275×183), similarly Fig.3(b) considered is of the size (75×111). As a result of application of Hessian matrix, the Eigen values are obtained. Using (3) and (4),  $F_{\text{structure}}$  and  $F_{\text{sheet}}$  that describe the characteristics of the image are obtained. From these two parameters, the similarity index  $S_{\text{fissure}}$  is determined from (5).

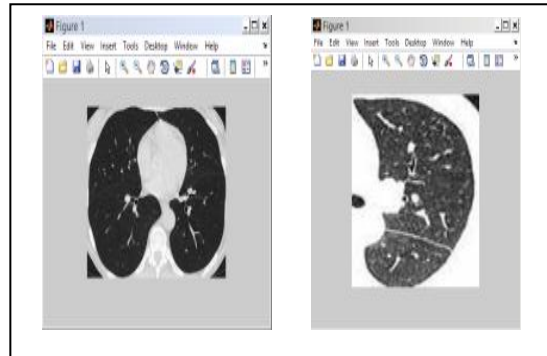


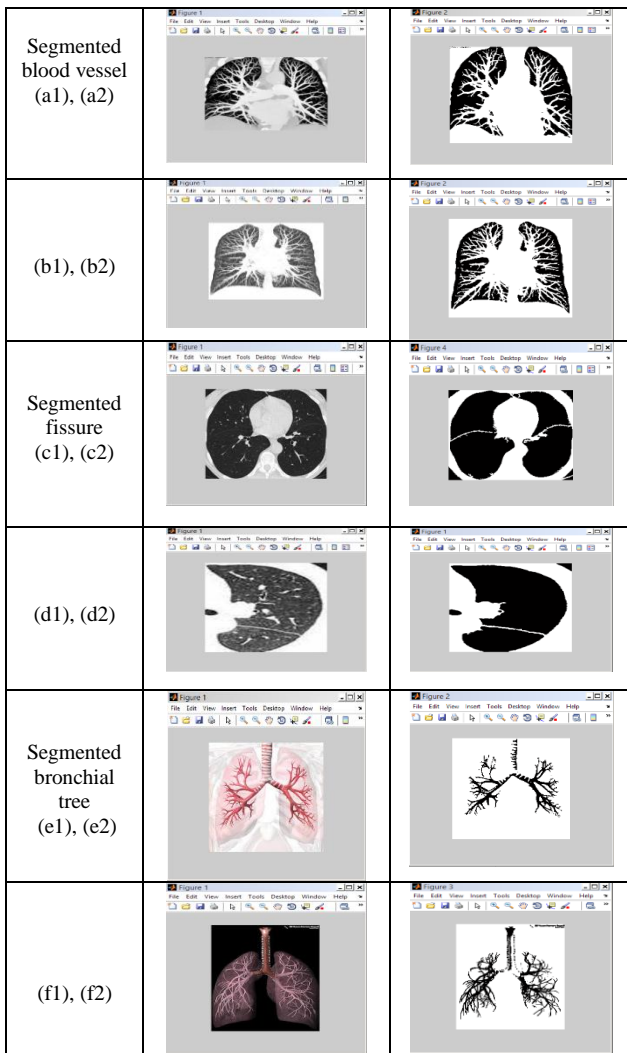
Fig.3(a),(b) images showing incomplete fissures

Table I. Fissure Enhancement Parameters

Figure	Parameters				
	$\lambda_2$	$\lambda_3$	$F_{\text{structure}}$	$F_{\text{sheet}}$	$S_{\text{fissure}}$
3(a)	27.09	40.04	0.994	0.198	0.197
3(b)	24.95	45.66	0.999	0.741	0.74

Table 1 shows the enhancement parameters of the Fig.3(a) and Fig.3(b), which is used for fissure segmentation. In both the cases,  $\lambda_3$  value lies above 30, hence the probability of being fissure is high. Similarly, while considering  $\lambda_2$ , if the value is between 0 and 30, the identified feature is discriminated as fissure. Also the parameter  $S_{\text{fissure}}$  lies in the range [0, 1].

Fig.4 Results obtained after segmentation



The Fig.4(a1), Fig.4(b1) shows the coronal screen shot of the lung image. This sample image, Fig 4(a1) is of the size (228×215), similarly Fig.4(b1) is of size (265×190). Both these images are rescaled to (255×255). After rescaling thresholding is applied with a threshold value 130, which is determined from the histogram analysis. The Fig.4(a2), Fig.4(b2), shows the segmented output of blood vessels. The Fig.4(c1), Fig.4(d1) shows the axial view of the lung image. The sample image Fig.4(c1) considered is of size (275×183), similarly Fig.4(d1) considered is of size (75×111). Based on the enhancement parameters from Table 1, mask C is obtained from the (6), which yields the segmented fissure output, which is shown in Fig.4(c2), Fig.4(d2). Fig.4(e1), Fig.4(f1) shows the 3-D view of lung image. Fig.4(e1) is of the size (227×222) and Fig.4(f1) is of the size (194×259). These images are first smoothed, and the blurred image is enhanced. For enhanced image, region growing technique is applied. This image is finally threshold by 90, to obtain

the segmented image, which is shown in Fig.4(e2) and Fig.4(f2).

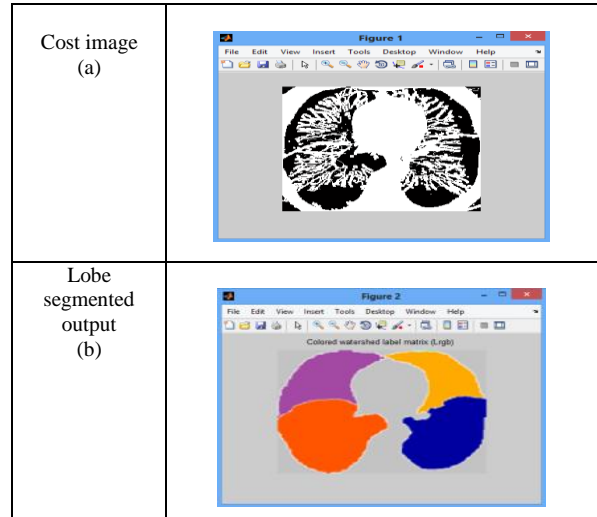


Fig.5 Cost image formation and lobe segmentation

The three segmented images are combined into cost image using fusion technique, which is the input for the lobe segmentation process. Fig.5(a) shows the cost image formed. Fig.5(b) shows the lobe segmented image of the lung. The selection of markers is the first primitive step in watershed algorithm, which helps to avoid over segmentation. Subsequently watershed algorithm is applied to obtain the segmented lung lobe. Fig.5(b) shows the final segmented output.

The proposed lung lobe segmentation method was applied to dataset 1 images. The mean was calculated for each lobar border. Table 2 shows the mean calculation and comparison with the existing methods by Van Rikxoort et al which show automatic segmentation robust against incomplete fissures [4] and Kuhnigk et al which proposed new tools for computer assistance in thoracic CT.

Table II. Results Showing Mean of Various Methodologies

Methods	Mean
Fissure alone is considered for Segmentation of Lobe	2.78
Cost Image using Euclidean Distance and ROI	1.08
Proposed Method	0.86

From the Table II, it is clear that the proposed method shows better performance than the existing methods like Rikxoort and Kuhnigk.

The proposed system is robust against incomplete fissure, but in cases of missing fissure the lobar boundary

is not exactly defined. The accuracy is determined from (7)

$$\text{Accuracy} = (\text{TP} + \text{TN}) / (\text{P} + \text{N}) \quad (7)$$

Where TP (True positive) and TN (True negative) are determined from the confusion matrix and P (Positive) and N (Negative) are estimated from the ground truth. Table III shows the accuracy calculation of the proposed methodology. A set of twenty images with incomplete fissure and missing fissure is considered for the accuracy calculation. Out of all 100 lobes in twenty images 84 was correctly segmented.

Table III. Accuracy Calculation

Number of Images Taken for Analysis	Total Number of Lobes	Number of Lobes Correctly Segmented	Accuracy (%)
25	125	105	84%

Table IV. Run Time Analysis

Schemes	Run time/ lung
Manual	75 min
Implicit surface fitting	25-30 min
Atlas based method	15 min
Proposed method	10 min

The run time measures are tabulated here. Table IV shows the comparison of the proposed algorithm and the existing algorithms like atlas based, implicit surface fitting [10]. The run time is considerably reduced when compared to the existing methods.

#### IV. CONCLUSION

This paper presents, an algorithm for automatic segmentation of lung lobe, which is robust against incomplete fissures. Fissures or lobar boundaries play a major role in diagnosing the lung disease. Nowadays, lung cancer is popularly seen among the people. Due to lung cancer the lung gets severely damaged. In such cases of severely affected lung, the fissures are incomplete. This algorithm performs lung lobe segmentation which overcomes the defect of exciting by including features like pulmonary vessels and bronchial tree.

#### REFERENCES

- [1] E. van Rikxoort, B. van Ginneken, M. Klik, and M. Prokop, "Super-vised enhancement filters: Application to fissure detection in chest CT scans," *IEEE Trans. Med. Imag.*, vol. 27, no. 1, pp. 1–10, Jan. 2008.
- [2] J. Pu, J. Leader, B. Zheng, F. Knollmann, C. Fuhrman, F. Sciuuba, and D.Gur, "A computational geometry approach to automated pulmonary fissure segmentation in CT examinations," *IEEE Trans. Med. Imag.*, vol. 28, no. 5, pp. 710–719, May 2009
- [3] E. M. van Rikxoort, B. de Hoop, S. van de Vorst, M. Prokop, and B. van Ginneken, "Automatic segmentation of pulmonary segments from volumetric chest CT scans," *IEEE Trans. Med. Imag.*, vol. 28, no. 4, pp. 621–630, Apr. 2009.
- [4] E. van Rikxoort, M. Prokop, B. de Hoop, M. Viergever, J. Pluim, and B. van Ginneken, "Automatic segmentation of pulmonary lobes robust against incomplete fissures," *IEEE Trans. Med. Imag.*, vol. 29, no. 6, pp. 1286–1296, Jun. 2010
- [5] S. Ukil and J. M. Reinhardt, "Anatomy-guided lung lobe segmentation in x-ray CT images," *IEEE Trans. Med. Imag.*, vol. 28, no. 2, pp. 202–214, Feb. 2009.
- [6] B. Lassen, J.-M. Kuhnigk, O. Friman, S. Krass, and H.-O. Peitgen, "Automatic segmentation of lung lobes in CT images based on fissures, vessels, and bronchi," *Proc. Int. Symp. Biomed. Imag.*, pp. 560–563, 2010.
- [7] Bianca Lassen, Eva M. van Rikxoort, Michael Schmidt, Sjoerd Kerkstra, Bram van Ginneken, and Jan-Martin Kuhnigk, "Automatic Segmentation of the Pulmonary Lobes From Chest CT Scans Based on Fissures, Vessels, and Bronchi" *IEEE Trans. Med. Imag.*, Vol. 32, no. 2, Feb 2013 .
- [8] Jiri Hladuvka, Andreas Konig, Edward Groller, "Exploiting Eigenvalues of the Hessian Matrix for Volume Decimation", Institute of computer Graphics and Algorithms, Vienna University of Technology, Karlsplatz 13/186, A-1040 Wien, Austria.
- [9] P. Spureka, A. Chaikouskayaa, J. Tabora, E. Zaja,cb, "A local Gaussian filter and adaptive morphology as tools for completing partially discontinuous curves", arXiv:1311.7430v1 [cs.GR] 28 Nov 2013.
- [10] S. Arastehfar1, A. A. Pouyan2\*, A. Jalalian1, "An enhanced median filter for removing noise from MR images", *Journal of AI and Data Mining* , Vol.1, No.1, 2013, 13-17.
- [11] Huiyan Jiang,1,2 Baochun He,1 Di Fang,1 Zhiyuan Ma,1 Benqiang Yang,3 and Libo Zhang3, "A Region Growing Vessel Segmentation Algorithm Based on Spectrum Information", *Computational and Mathematical Methods in Medicine* Volume 2013, Article ID 743870, 9 pages.
- [12] H.P. Narkhede, "Review of Image Segmentation Techniques", *International Journal of Science and Modern Engineering (IJISME)* ISSN: 2319-6386, Volume-1, Issue-8, July 2013.
- [13] Rohan Ashok Mandhare, Pragati Upadhyay, Sudha Gupta, "Pixel-Level Image Fusion Using Brovey Transform And Wavelet Transform", *International Journal of Advanced Research in Electrical, Electronics and Instrumentation Engineering* , Vol. 2, Issue 6, June 2013
- [14] B.Sridhar, Dr.K.V.V.S.Reddy, Dr.A.M.Prasad, "Automated Medical image segmentation for detection of abnormal masses using Watershed transform and Markov random fields", *ACEEE Int. J. on Signal and Image Processing* , Vol. 4, No. 3, Sept 2013.
- [15] D. Selle, B. Preim, A. Schenk, and H.-O. Peitgen, "Analysis of vasculature for liver surgical planning," *IEEE Trans. Med. Imag.*, vol. 21, no. 11, pp. 1344–1357, Nov. 2002.